Received: 6 June 2018 | Revised: 20 November 2018 | Accepted: 28 November 2018

DOI: 10.1002/hbm.24495

WILEY

RESEARCH ARTICLE

Oscillatory dynamics of cortical functional connections in semantic prediction

Fahimeh Mamashli[1] | Sheraz Khan[1] | Jonas Obleser[2] | Angela D. Friederici[3] | Burkhard Maess[4]

[1]Department of Radiology, Massachusetts General Hospital, Athinoula A. Martinos Center for Biomedical Imaging, Harvard Medical School, Boston, Massachusetts

[2]Department of Psychology, University of Lübeck, Lübeck, Germany

[3]Department of Neuropsychology, Max Planck Institute for Human Cognitive and Brain Sciences, Leipzig, Germany

[4]MEG and Cortical Networks Group, Max Planck Institute for Human Cognitive and Brain Sciences, Leipzig, Germany

Correspondence
Fahimeh Mamashli, 149 13th Street, Charlestown, MA 02129.
Email: fmamashli@mgh.harvard.edu

Funding information
Elekta Oy; Nancy Lurie Marks Family Foundation; International Max Planck Research School Leipzig; Max Planck Society

Abstract

An event related potential, known as the N400, has been particularly useful in investigating language processing as it serves as a neural index for semantic prediction. There are numerous studies on the functional segregation of N400 neural sources; however, the oscillatory dynamics of functional connections among the relevant sources has remained elusive. In this study we acquired magnetoencephalography data during a classic N400 paradigm, where the semantic predictability of a fixed target noun was manipulated in simple German sentences. We conducted inter-regional functional connectivity (FC) and time–frequency analysis on known regions of the semantic network, encompassing bilateral temporal, and prefrontal cortices. Increased FC was found in less predicted (LP) nouns compared with highly predicted (HP) nouns in three connections: (a) right inferior frontal gyrus (IFG) and right middle temporal gyrus (MTG) from 0 to 300 ms mainly within the alpha band, (b) left lateral orbitofrontal (LOF) and right IFG around 400 ms within the beta band, and (c) left superior temporal gyrus (STG) and left LOF from 300 to 700 ms in the beta and low gamma bands. Furthermore, gamma spectral power (31–70 Hz) was stronger in HP nouns than in LP nouns in left anterior temporal cortices in earlier time windows (0–200 ms). Our findings support recent theories in language comprehension, suggesting fronto-temporal top–down connections are mainly mediated through beta oscillations while gamma band frequencies are involved in matching between prediction and input.

KEYWORDS

functional connectivity, language, MEG, N400, oscillation, prediction, semantics

1 | INTRODUCTION

Language comprehension requires decoding of highly structured speech signals within a very short time (Friederici, 2002; Hickok & Poeppel, 2007; Pylkkanen & Marantz, 2003; Scott, Blank, Rosen, & Wise, 2000). Yet, healthy humans can comprehend up to 210 words per minute without any loss (Omoigui, He, Grudin, & Sanocki, 1999). A potential explanation for this speed and efficiency is that our brains may make predictions about upcoming linguistic input. This idea is supported by many studies suggesting that prediction is employed during language processing (Federmeier & Kutas, 1999; Grisoni, Miller, & Pulvermuller, 2017; Kamide, Scheepers, & Altmann, 2003; Knoeferle, Crocker, Scheepers, & Pickering, 2005; Maess, Mamashli, Obleser, Helle, & Friederici, 2016; McRae, Hare, Elman, & Ferretti, 2005; Van den Brink, Brown, & Hagoort, 2001; Van Petten, Coulson, Rubin, Plante, & Parks, 1999). Particularly, lexical semantic prediction has been investigated using the so-called N400 paradigm which was first described by Kutas and Hillyard (1980b) who discovered using EEG when participants read sentences that unexpected words at the end (i.e., *I take coffee with cream and dog*) elicit a negative event-related potential (ERP) at about 400 ms. Reduced N400 responses have been reliably observed for words in a predictive or supportive context (Federmeier, 2007; Kutas & Federmeier, 2011; Kutas & Hillyard, 1980a, 1984; Lau, Almeida, Hines, & Poeppel, 2009; Lau, 2009; Lau, Holcomb, & Kuperberg, 2013; Wlotko & Federmeier, 2012). Furthermore, it has been demonstrated that the N400

amplitude inversely correlates with the predictability of the word within the given context (DeLong, Urbach, & Kutas, 2005).

A theoretical framework on efficient information processing is the predictive coding theory, which postulates that the brain is hierarchically organized (Felleman & Van Essen, 1991; Mumford, 1992) and continuously anticipates upcoming events by sending predictions from higher to lower hierarchical levels via feedback connections (Clark, 2013; David & Friston, 2003; Friston, 2005; Friston, Kilner, & Harrison, 2006; Helmholtz, 1925; Huang & Rao, 2011; Rao & Ballard, 1999; Srinivasan, Laughlin, & Dubs, 1982; Swanson, 2016). Furthermore, predictive coding assumes that prediction errors, that is, the difference between inputs and predictions, are sent from lower to higher cortical levels via feedforward connections. Recently, studies on language comprehension have attempted to model information processing under predictive coding theory (David, Maess, Eckstein, & Friederici, 2011; Hickok, 2012; Jakuszeit, Kotz, & Hasting, 2013; Lewis, Schoffelen, Schriefers, & Bastiaansen, 2016; Park, Ince, Schyns, Thut, & Gross, 2015; Sohoglu, Peelle, Carlyon, & Davis, 2012). A predictive coding model of single spoken word recognition, proposed by Gagnepain, Henson, and Davis (2012), suggests that superior temporal gyrus (STG) neurons represent the difference between predicted and heard speech sounds.

In our previous article, we proposed a simplified version of the predictive coding model on N400 generation (Maess et al., 2016). Here, we briefly recapitulate our hypothesis. Consider a sentence "he drives the car" in which the target noun "car" is highly predicted (HP) by the previous verb "drives." We assume that prediction $\widetilde{X}$ is generated for the word "car," prior to its presentation, and based on predictive coding theory, $\widetilde{X}$ is conveyed from higher to lower cortical areas. As a result, processing of the word "car" requires only the difference, between "car" and $\widetilde{X}$ to be fed forward up the processing hierarchy. Smaller differences between prediction $\widetilde{X}$ and actual input, means less bottom–up information transfer and fewer adjustments required at the higher level, thus, less top–down processing too. Now, consider another sentence "he gets the car" in which the noun is less predicted (LP) given the previous verb. In this case, accurate predictions are unlikely to be generated and all information in the word "car" must be conveyed from lower to higher levels after it is presented. More processing at the higher level would be required as the noun "car" now provides the information, which was missed until that point. Therefore, when we compare the hierarchical information flow for the word "car" in HP and LP conditions, we would generally expect less processing in HP than LP. This means we expect less top–down and less bottom–up processing in HP than LP condition. We have illustrated our hypothesis in Figure 1.

In addition, recent studies suggest a strong link between the predictive coding account of hierarchical information flow and the oscillatory neural dynamics in the brain (Arnal & Giraud, 2012; Arnal, Wyart, & Giraud, 2011; Bastos et al., 2012; Cannon et al., 2014; Engel & Fries, 2010; Kopell, Ermentrout, Whittington, & Traub, 2000; Wang, 2010). Specifically, empirical studies on rats (Kopell et al., 2000), monkeys (Bastos et al., 2015), and humans (Arnal et al., 2011) suggest that hierarchical information flow via feedback- and feedforward-connections are mediated through distinct frequency bands. It is proposed that top–down processing is preferentially mediated through beta band oscillations whereas bottom–up processing is propagated through gamma oscillations (Bastos et al., 2012, 2015; Khan et al., 2018; Obleser, 2016; Sedley et al., 2016; Wang, 2010).

Adopting the predictive coding view to language comprehension, Lewis and Bastiaansen (2015) proposed a double role of beta oscillations in maintaining certain cortical network configurations during sentence-level processing and in the top–down propagation of prediction to hierarchically lower levels. Low- and middle evoked gamma (35–75 Hz) has been suggested to reflect the matching of bottom–up and top–down information, while high evoked gamma (80–130 Hz) may reflect the propagation of bottom–up prediction errors (Lewis et al., 2016). Recently, Schoffelen et al. (2017) estimated granger causality between cortical areas as subjects read word sequences and observed that connections originating from frontal areas peaked in the beta band whereas connections originating from temporal areas peaked in the alpha band. This beta band granger causality from frontal areas may represent top–down information transfer, consistent with the Lewis and Bastiaansen (2015) model. Frontal areas, including orbitofrontal and inferior frontal, have been linked to higher order processing in general (Badre, Poldrack, Pare-Blagoev, Insler, & Wagner, 2005; Badre & Wagner, 2007; Engel, Fries, & Singer, 2001) and to language comprehension in particular (Martin, 2007; Thompson-Schill, D'Esposito, & Kan, 1999). Alpha band granger causality originating from temporal areas may indicate bottom–up processing, which is in contrast to the Lewis and Bastiaansen (2015) model associating alpha band with feedback signaling and top–down influence.

The goal of the current study is to investigate hierarchical information flow in N400 generation. We tested our hypothesis based on predictive coding following the proposal of Lewis and Bastiaansen (2015). Previous studies have shown that synchronization between cortical areas may indicate communication between those areas, with the phase locking values as a measure of synchrony (Doesburg, Kitajo, & Ward, 2005; Fries, 2005, 2015; Panagiotaropoulos, Deco, Kapoor, & Logothetis, 2012; Pantazis et al., 2017; Tallon-Baudry & Bertrand, 1999; Weeks et al., 1999). Phase locking values were estimated between cortical areas involved in semantic processing. It should be noted that phase-locking values do not estimate the directionality of the information flow between cortical areas. We chose this approach, in particular, because it is a data driven method. In contrast, model driven approaches such as dynamic causal modeling or granger causality are useful in estimating the directionality of the connectivity. However, they require assumptions of the temporal and spatial covariance of the sources that are difficult to estimate in the presence of noise and with a limited amount of data. We are conducting this study to understand the connectivity dynamics between areas involved in semantic prediction, specifically in terms of spectral and temporal characteristics. So far, the majority of N400 studies have focused on varying linguistic parameters and identifying the neural sources, however, the communication between those sources in time and frequency is largely unknown.

We used data from a classic N400 paradigm in which identical target nouns were either HP or LP. An earlier publication describes

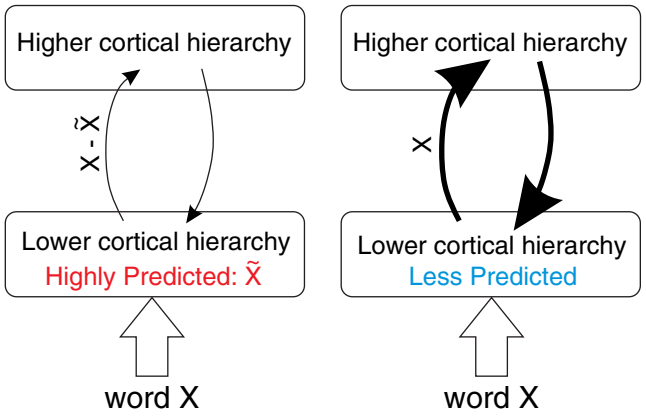

FIGURE 1 Illustration of top–down and bottom–up information flow when the word X is highly predicted and less predicted. The strength of the arrows schematically represents the amount of top–down and bottom–up processing. For generalizability, we use the term "X" to represent a word [Color figure can be viewed at wileyonlinelibrary.com]

the analysis of the evoked magnetic fields of the same data (Maess et al., 2016). In this article, we focus on spectrally resolved, functional connectivity measures to track the information transfer between brain areas.

2 | MATERIALS AND METHODS

2.1 | Stimuli

Stimuli were short German sentences, which were grouped based on the cloze probability values, that is, the probability that mother tongue speakers would select this word to complete the given context (Taylor, 1953). Nouns which had a cloze probability greater than 50% were considered as having high semantic predictability (HP), [e.g., *He drives the car, German: Er fährt das Auto*] and those with a cloze probability less than 24% were considered to have low semantic predictability (LP), [e.g., *He gets the car, German: Er kriegt das Auto*] (Maess et al., 2016). Each condition consisted of 69 items. Sentences were spoken by a trained female speaker at natural speed. Loudness was adjusted so that all sentences were presented at the same volume.

2.2 | Participants

Twenty-one German native speakers (11 female) participated in a Magnetoencephalography (MEG) experiment (age range: 20–32 years, median: 27). All were right-handed according to the Edinburgh Handedness Inventory (Oldfield, 1971). None of the participants had a hearing deficit or neurological disease. Participants gave written informed consent prior to the experiment and were paid for their participation. The study followed the guidelines of the declaration of Helsinki and received ethical approval from the ethics commission of the University of Leipzig (Ref. 059-11-07032011).

2.3 | Design and procedure

Participants were seated in a dimly lit shielding room (Vacuumschmelze Hanau, Germany). MEG data was recorded with a 306 channel Vectorview device (Elekta, Helsinki, Finland) at 500 Hz sampling rate utilizing a bandwidth of 160 Hz. The experiment was conducted in one session with five recording blocks. First, participants' individual hearing thresholds were determined for both ears separately. Stimuli were presented at 48 dB SL (sensation level, i.e., above the mean individual hearing threshold). Sensation level was estimated using a subpart of one of the sentences. For the first two blocks stimuli were randomized and presented once, thereafter presentation of all stimuli was repeated in blocks 3 and 4, using a different randomization to increase the number of trials and consequently signal to noise ratio. Therefore, 138 stimuli per condition were presented in total. The onsets of all sentences, as well as the onsets of the verbs and the nouns in each sentence, were specifically marked. During the fifth block, a sequence of simple tones (200 ms length and 500 Hz pitch) were presented, with a stimulus onset asynchrony (SOA) of 2,200 ms, at the same loudness level as the sentence stimuli to provide data to control for the accuracy of the MEG inverse solutions.

Participants were instructed to listen carefully to the presented sentences and not to move during a block. They were asked to fixate a visually projected cross while listening to the auditory stimulation. Fixation crosses were presented from 700 ms before onset until 700 ms after the offset of each sentence. Fifteen percent of the sentences were followed by the same, or an alternative sentence, spoken by a male. Participants' (incidental) task was to judge whether the two preceding sentences (female and male voice) were the same. Participants responded by a button press following the cue. The cue also informed participants of the response-to-button-alignment: It was comprised of one happy and one sad symbolic face (smiley), one presented on the left side of the screen and the other on the right side of the screen. Participants had to use their thumbs to press either the left or the right side button, that is, giving the answer "yes" with the button at the side of the happy face and "no" with the other. The arrangement of the faces on the screen was randomized and counterbalanced over all stimuli in each block.

2.4 | Data preprocessing

The MEG data were spatially filtered using the signal space separation (SSS) method (Elekta-Neuromag Maxfilter software) to suppress environmental interference (Taulu, Kajola, & Simola, 2004; Taulu & Simola, 2006). SSS was further used to transform the data from each block into the same head position (Taulu et al., 2004). Cardiac and ocular artifacts were removed by signal space projection (Gramfort et al., 2014). MEG data were filtered with a low pass filter of 90 Hz using MNE-C (fft based filter) with a filter size of 8,192. Data were epoched into single trials lasting 1.4 s, extending from 400 ms before noun onset to 1,000 ms following it. For baseline correction purposes in the time-frequency analysis, data were epoched from −400 to 400 ms time-locked to the sentence onset. The baseline interval is taken as point of reference for the spectral power estimates as it by design represents no condition difference. This baseline includes the first stages of acoustic processing but no generation of linguistic predictions as all sentences begin identically. Using this baseline allows us to separate linguistic stages from pure acoustic processing

stages. Epochs were rejected if the peak-to-peak amplitude exceeded 150 μV, 1 pT/cm, and 3 pT in any of the electrooculogram, gradiometer, and magnetometer channels, respectively. To achieve a similar signal-to-noise ratio in each condition (i.e., HP and LP), the number of trials in the lesser populated condition was used to analyze both conditions. To this end, trials from the more numerous conditions were randomly selected from the reservoir of acceptable trials. After artifact rejection the mean number of trials per condition was 99 when averaging over subjects. The subject with the smallest number of trials provided 72 trials per condition.

2.4.1 | Source estimation

The geometry of each participant's cortical surface was reconstructed from 3D structural MRI data using FreeSurfer software (http://surfer.nmr.mgh.harvard.edu). The cortical surface was decimated to a grid of 10,242 dipoles per hemisphere, corresponding to a spacing of approximately 5 mm between adjacent source locations on the cortical surface. The MEG forward solution was computed using a single-compartment boundary-element model (BEM) assuming the shape of the intracranial space (Hämäläinen & Sarvas, 1987). The watershed algorithm was used to generate the inner skull surface triangulations from the T1-weighted MR images of each participant. The cortical current distribution was estimated using a depth-weighted, minimum-norm estimate (MNE) (http://www.martinos.org/martinos/userInfo/data/sofMNE.php [Lin, Belliveau, Dale, & Hämäläinen, 2006]) assuming a fixed orientation of the source, perpendicular to the individual cortical mesh. The noise-covariance matrix used to calculate the inverse operator was estimated from data collected from empty room recordings prior and following the recordings with each subject. To reduce the bias of the MNEs toward superficial currents, we used depth weighting, that is, the source covariance matrix was adjusted to favor deep source locations.

2.4.2 | Inter-subject cortical surface registration for group analysis

Each participant's inflated cortical surface was registered to an average cortical representation (FsAverage in FreeSurfer) by optimally aligning individual sulcal–gyral patterns computed in freesurfer (Fischl, Sereno, & Dale, 1999). We employed a surface-based registration technique based on folding patterns because it provides more accurate inter-subject alignment of cortical areas than volume-based approaches (Fischl, Sereno, Tootell, & Dale, 1999; Van Essen & Dierker, 2007).

2.4.3 | Regions of interest identifications and analysis

Regions of interest (ROI) were selected from the Freesurfer parcellation (Desikan–Killiany Atlas) and covered seven areas spanning both hemispheres known to be parts of the network for semantic language processing (Friederici, 2011; Lau, Phillips, & Poeppel, 2008; Maess et al., 2016; Price, 2010), namely bilateral superior temporal gyrus (STG), middle temporal gyrus (MTG), inferior frontal gyrus (IFG) including Brodmann areas BA44, BA45, and BA47 and left lateral orbitofrontal cortex (LOF) in agreement with our previous article (Maess et al. 2016). However, here we selected only ROIs from the lateral side of the cortex and ignored the deeper, medial part because of the poor SNR of the deeper source (Ahlfors, Han, Belliveau, & Hamalainen, 2010). In addition, we used an automatic routine (mris_divide_parcellation) available in the Freesurfer package (equal size principle) to break each large ROI into smaller equal size sub-ROIs; that is, all sub-ROIs in all ROIs were of approximately the same size—thereby increasing the spatial specificity for further connectivity analysis. Large ROIs can lead to temporal signal cancelations.

2.4.4 | Sub-ROI time series extraction

Epochs were extracted for all vertices within each sub-ROI. Epochs were averaged across vertices to compute the mean sub-ROI time course, generating $\boldsymbol{X}(\Lambda, T, N)$, where Λ is the number of vertices, T is the number of time points and N is the number of epochs. Owing to the ambiguity of individual vertex (dipole) orientations, these time series were not averaged directly but first aligned with the dominant component of the multivariate set of time series, before calculating the sub-ROI mean. In order to align the sign of the time series across vertices we first concatenated all the epochs for all sub-ROI vertices in a matrix of the dimension [vertices × samples] conducted an SVD of it $\mathbf{X}^{\mathrm{T}} = \mathbf{U}\boldsymbol{\Sigma}\mathbf{V}^{\mathbf{T}}$. If the sign of the dot product between the first left singular vector U and a time series was negative, we inverted the time-series before averaging over all vertices resulting in a 2D matrix [epochs × time] per sub-ROI.

2.4.5 | Time frequency decomposition

In a next step, each epoched time series was convolved with a dictionary of complex Morlet wavelets, transforming the real 2D matrices into complex 3D matrices **S** [epochs × time × frequency]. The number of cycles used in the Morlet wavelets varied as a function of frequency as follows: 8–30 Hz: 7 cycles and 31–70 Hz: 9 cycles. The same time-frequency decomposition was conducted for both analyses, time-locked to the noun onset from −400 to 1,000 ms and to the sentence onset from −400 to 400 ms.

2.4.6 | Functional connectivity computation

We used the inter-trial phase-locking value (PLV), to estimate the connectivity between ROIs. The PLV measures the consistency of phase differences between two ROIs across epochs (Lachaux, Rodriguez, Martinerie, & Varela, 1999). Here we use the term for two ROIs (I, J) and the corresponding sub-ROIs (i, j) represented as I_i, J_j, respectively. Separately for both conditions, PLV was estimated between each sub-ROI pair (I_i, J_j) in $\mathrm{ROI_I}$ and $\mathrm{ROI_J}$, ($1 \le I \le \kappa - 1$, $I < J \le K$, $K = 7$) for all frequencies between 8 and 70 Hz and latencies:

$$PLV_{I_i,J_j}(t,f) = \frac{1}{N}\left|\sum_{n=1}^{N} e_n^{\left(\emptyset(f,t)_{I_i} - \emptyset(f,t)_{J_j}\right)}\right|$$

K is the number of ROIs, $i = 1, \ldots, \Upsilon$, $j = 1, \ldots, \ell$. Υ, ℓ are the maximum number of sub-ROIs in $\mathrm{ROI_I}$ and $\mathrm{ROI_J}$, respectively. In order to eliminate the statistical bias due to the non-Gaussian distribution of phase-locking values and the problem of spurious connectivity (Sekihara, Owen, Trisno, & Nagarajan, 2011), we used normalized phase-locking values, sometimes also referred to as ZPLV (Maris, Schoffelen, & Fries, 2007). In this measure, the principal condition (LP with (N_1=70) epochs) is normalized with respect to a baseline condition (HP with

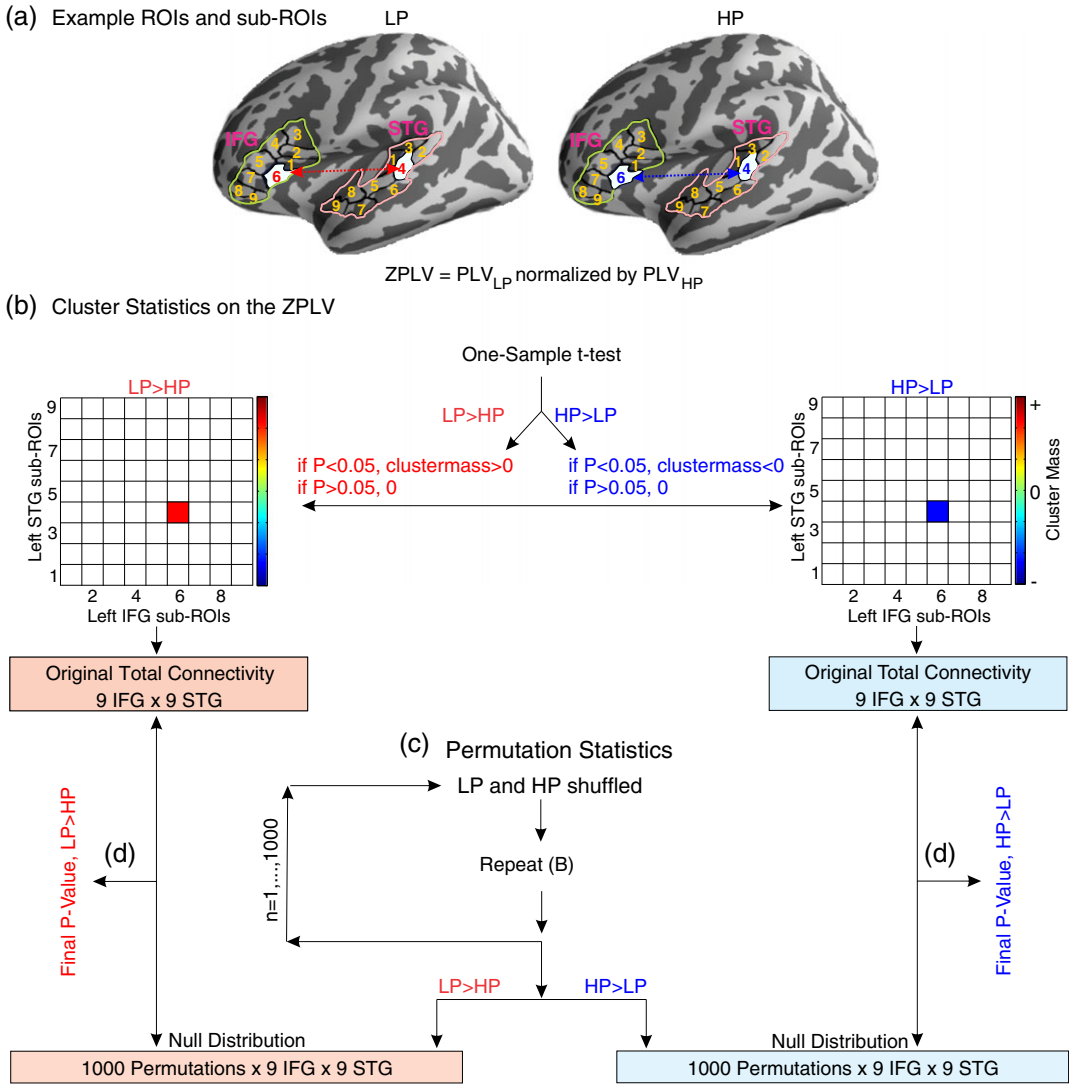

FIGURE 2 A schematic display of the statistical analysis for the comparison of functional connectivity between LP and HP conditions. (a) Two example ROIs are considered in left STG and IFG. ZPLV was computed for each sub-ROI connection, with Υ = 9 and ℓ = 9 maximum number of sub-ROIs. (b) Cluster-based statistics using one sample *t*-tests were done on the ZPLV values across all subjects at each sub-ROI pair. Two 2D matrixes were generated based on the *p*-values and the sign of cluster masses. (c) LP and HP data were permuted and the cluster statistics repeated 1,000 times to generate the null distribution. (d) Two *p*-values were assigned for LP > HP (left panel) and HP > LP (right panel) by comparing the original total connectivity with the null distribution [Color figure can be viewed at wileyonlinelibrary.com]

(N_2 = 70) epochs), which addresses the bias (e.g., Khan et al., 2013), (Figure 2):

$$ZPLV_{l_i,J_j}(t,f) = \sqrt{\frac{N-2}{2}}\left(\tanh^{-1}\left(\left|PLV^{LP}_{l_i,J_j}(t,f)\right|\right) - \tanh^{-1}\left(\left|PLV^{HP}_{l_i,J_j}(t,f)\right|\right)\right)$$

"*N*" represents the number of epochs. Note that the *ZPLV* formula is simplified from Maris et al. (2007) because, in our case, $N_1 = N_2$.

2.4.7 | Power computation

A. Temporally resolved power estimates were separately averaged over epochs for both conditions, each subject and each sub-ROI. Averaged power changes in the post stimulus interval (0–700 ms) were estimated as relative change from the baseline interval (averaged power of both conditions at sentence onset: −300 to −100 ms). The aim of this analysis was to find out the potential confounding effect of power on connectivity results.

B. For the early time interval (no temporal resolution): Following our hypothesis for the early gamma effect, an additional power estimate was computed specifically for the time interval of 0–200 ms from the noun onset in STG and MTG. To this end, we applied Welch's method (with Hann window, window size = 200 ms) (Hayes, 1996; Stoica & Moses, 1997). We used the same baseline power reference as in (A).

2.4.8 | Statistical analysis of functional connectivity: Correction in time, frequency and space

All statistics on the ZPLV, were carried out in three steps, focused in time from 0 to 700 ms with increments of 2 ms, and frequencies from 8 to 70 Hz selected on a 34-point logarithmic scale (Kitzbichler et al., 2015). The analysis strategy is depicted in Figure 2. This results in a very large number of comparisons calling for appropriate corrections. We selected two nonparametric methods to account for this. First, for

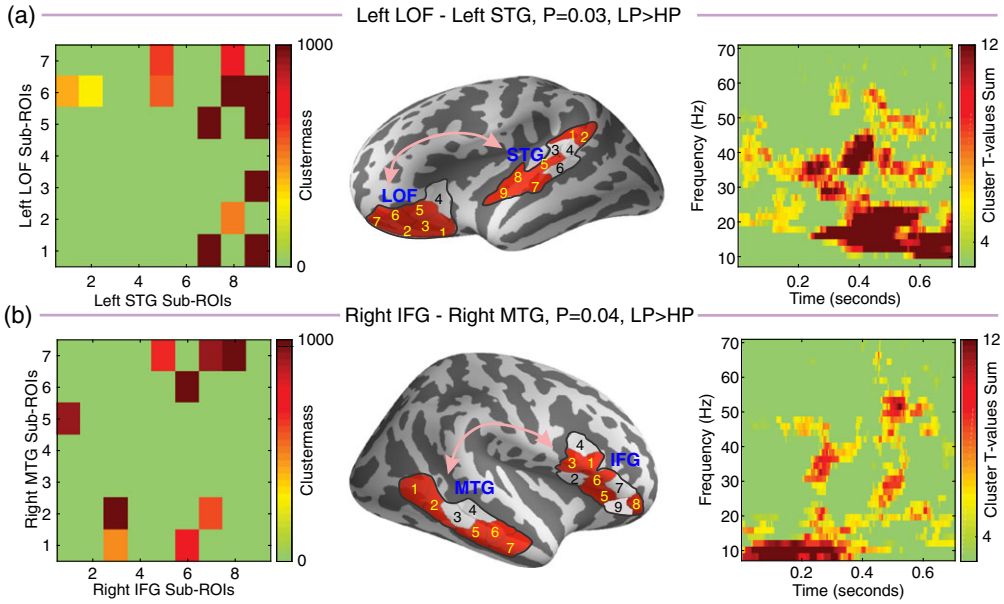

FIGURE 3 Functional connection between left LOF and left STG (a) and between right IFG and right MTG (b). For each panel, the left column is the matrix of sub-ROI pairs that reached significance; the middle column shows the sub-ROIs at the cortex, and the right column the time frequency map of the sum of the t-values inside the cluster masks between the significant sub-ROIs from the left column. In (a), the brain is rotated to show all sub-ROIs in LOF [Color figure can be viewed at wileyonlinelibrary.com]

each connectivity between a pair of sub-ROIs, cluster-based statistics were applied (Maris & Oostenveld, 2007). Second, statistical analysis over all pairs was conducted using random permutations. In step (1): We used $p < 0.05$ as the initial threshold, 1,000 permutations and one sample *t*-tests as the test statistics. Please note that the normalized phase locking value is a Z-score from the LP versus HP comparison, which is approximately normally distributed. The cluster statistic's output is a *p*-value, cluster mass, cluster mask, and the *t*-values, for each cluster. A *p*-value smaller than 0.05 indicates that the cluster is significant after multiple comparisons correction in time and frequency. The cluster mass is the sum of the *t*-values of all vertices inside the cluster; a positive cluster mass means LP > HP whereas negative means HP > LP. The cluster mask is a matrix with the same dimensions as the tested plane (time by frequency). Values of zero and one indicate which time and frequency bins belong or do not belong to a cluster, respectively. Two additional masks are also generated: One for the case LP > HP and a second for HP > LP. For significant clusters ($p < 0.05$), we used cluster masses in the 2D matrix (Figure 2b). At this stage we had a matrix with the size of $\Upsilon \times \ell$ corresponding to Υ sub-ROIs in ROI_I and ℓ sub-ROIs in ROI_J for LP > HP and a similar matrix for HP > LP (Figure 2b). The sum of the cluster masses of each significant pair of this $\Upsilon \times \ell$ matrix was called "original total connectivity". Step (2): In order to estimate the null distribution of this total normalized-connectivity, we randomly flipped the sign of ZPLV at the subject level, without repetition, and conducted the cluster statistics (LP vs. HP) at each (I_i, J_j) sub-ROI pair again. This step also corrected for multiple comparison in space (across all sub-ROIs) using maximum statistics (Figure 2c). By permuting LP and HP conditions' datas 1,000 times and repeating the cluster statistics, we ended up with a matrix of 1,000 permutation $\times\Upsilon \times \ell$ values as a null distribution for LP > HP and HP > LP. Step (3): The null distribution was compared with the nonpermuted original total connectivity of the $\Upsilon \times \ell$ matrix, resulting in one *p*-value for LP > HP and one for HP > LP corrected in time, frequency and space (Figure 2d).

In summary, multiple comparisons within each of the sub-ROIs are accounted for by the cluster analysis in time and frequency (Step 1) and by the permutations approach (Step 2, 3) for the sub-ROIs tests. Please see (Mamashli et al., 2017) for more details on this method. Matlab scripts are available online through our github repository (https://github.com/fm897/NSR). Note that, we ignored ROI-to-ROI connections that would link adjacent ROIs as between STG and MTG or left IFG and LOF. This is due to the fact that there is a strong point spread effect in nearby areas; therefore the results may not be reliable.

2.4.9 | Statistical analysis of power

A. With temporal resolution: Cluster statistics were used to compare the power between two conditions in time (0–700 ms) and frequency (8–70 Hz on a logarithmic scale with 34 steps) in each sub-ROI. We used $p < 0.05$ as the initial threshold, 1,000 permutations and paired t-tests to compare HP and LP conditions. Nonparametric methods were then applied to correct for multiple comparisons based on the number of sub-ROIs within each ROI.
B. For the early time interval (no temporal resolution): Gamma power (31–70 Hz) was averaged across all vertices within each sub-ROI and paired *t*-tests were used to compare the LP versus HP conditions. In order to correct for multiple comparisons across all sub-ROIs, FDR correction was applied for each ROI with $q = 0.05$.

3 | RESULTS

3.1 | Functional connectivity

We found significantly stronger functional connectivity for LP than HP in: left LOF-left STG ($p = 0.03$), right IFG-right MTG ($p = 0.04$), and left LOF-right IFG ($p = 0.04$). The time-frequency map of the

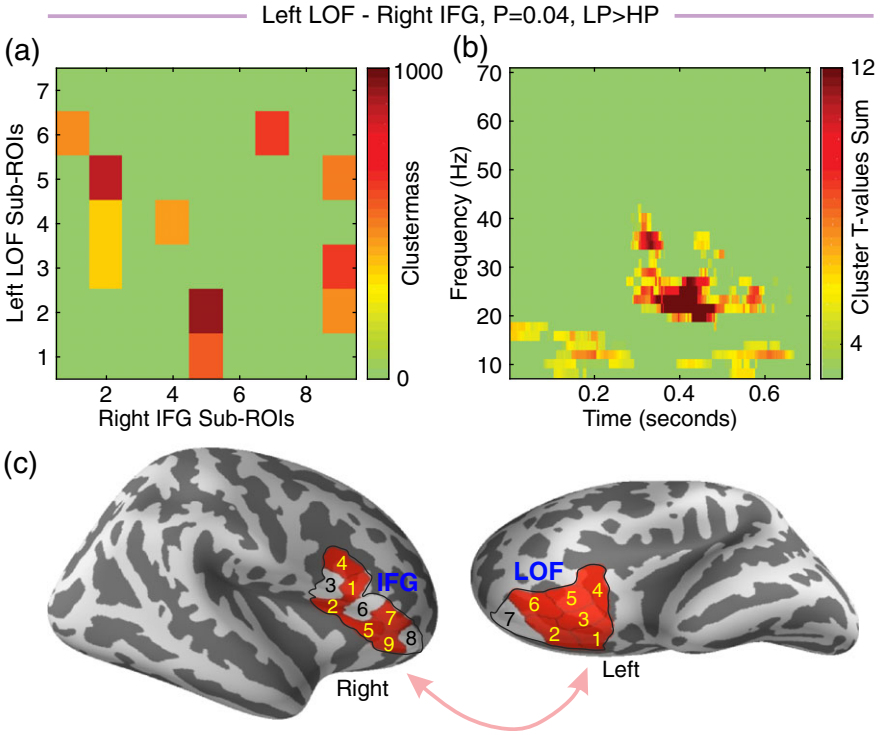

FIGURE 4 Functional connection between left LOF and right IFG. (a) Matrix of sub-ROI pairs that reached significance, (b) time frequency map of the sum of the t-values inside the cluster masks between the significant sub-ROIs from (a). (c) Sub-ROIs from a on the cortex. The brain in c showing LOF is rotated to show all sub-ROIs [Color figure can be viewed at wileyonlinelibrary.com]

conditional effect in these connections were as follows: In left LOF-left STG beta and low gamma band, from 300 to 700 ms, was predominant (Figure 3a), in right IFG-right MTG, the effect was earlier, from 0 to 350 ms, and mainly in lower frequencies (<15 Hz) with some distributed beta and low gamma (Figure 3b) and in left LOF-right IFG, the effect was in beta (20–30 Hz) frequency, around the 300–500 ms time interval (Figure 4). One connection showed a trend to be stronger in LP than HP: left LOF-right STG (p = 0.1). The primary effect in left LOF-right STG was in the beta band around 400 ms.

3.2 | Power

A. With temporal resolution: None of the ROIs showed a significant difference in power between the two conditions. The power findings are consistent with Wang, Zhu, and Bastiaansen (2012) in which no difference was found between LP and HP conditions.
B. For the early time interval (no temporal resolution): We found a significant gamma power (31–70 Hz) increase in the early time window from 0 to 200 ms, for the HP compared with LP condition, in left STG and MTG in anterior sub-ROIs (Figure 5). The same analysis did not yield any significant effects in any other ROIs.

4 | DISCUSSION

The goal of the current study was to investigate the rhythmic cortical interactions in semantic prediction and test the principles of predictive coding in language comprehension. To that end, we measured intercortical synchronization using phase locking values between bilateral superior and middle temporal, inferior frontal and left orbitofrontal. In general, the functional connectivity findings are consistent with our hypothesis, illustrated in Figure 1, supporting the predictive coding model of hierarchical information flow in semantic prediction. Increased PLVs were found for LP compared with HP in three connections: left LOF–left STG, right IFG–right MTG, and left LOF–right IFG. Interestingly, we found increased gamma power for the first 200 ms of noun processing in HP relative to LP, specifically in the left anterior STG and MTG.

Significant PLVs were observed for LP > HP between the left STG and the left LOF from about 300 ms onward, mainly in the beta and low gamma bands. Using transfer entropy, Park et al. (2015) showed top–down information transfer from left frontal areas to the auditory cortex in language processing. In addition, Cope et al. (2017) recently demonstrated a causal connection from the left frontal to the superior temporal area within beta band in predictive speech processing. Given the established role of the prefrontal and orbitofrontal cortex in higher order language comprehension (Halgren et al., 1994; Lau et al., 2008), our observation of larger PLVs for LP in the beta band between the left LOF and STG may represent a top–down role, in line with Lewis and Bastiaansen's model (Lewis & Bastiaansen, 2015). Increased beta band activity may also reflect the active maintenance of the cortical network configuration responsible for the construction and representation of the current sentence-level meaning (Lewis & Bastiaansen, 2015).

In addition, we observed increased low gamma band PLVs for LP compared with HP between the left STG and the left LOF from about 250 ms onward. Following our hypothesis of increased top–down and bottom–up processing in LP nouns, here the low gamma PLVs may represent stronger bottom–up information transfer from the left STG

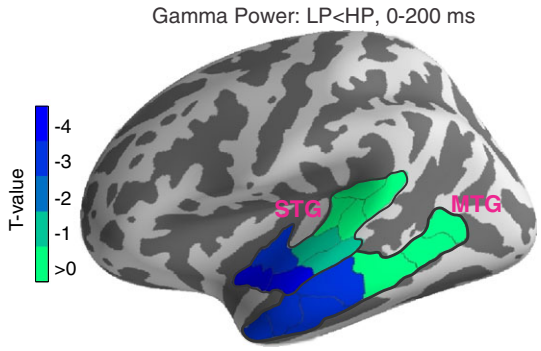

FIGURE 5 *T*-values for all sub-ROIs in left STG and MTG when comparing the gamma power between the two conditions in the time window (0–200 ms). Negative t-value means LP < HP. Sub-ROIs with *t*-values less than −2.2 are significant with FDR correction [Color figure can be viewed at wileyonlinelibrary.com]

to the left LOF required to process the LP nouns. This is consistent with the general theory of associating gamma oscillations with feedforward processing (Bastos et al., 2012, 2015; Khan et al., 2018; Obleser, 2016; Sedley et al., 2016; Wang, 2010). However, this has not been established in language processing literature. The majority of studies have focused on power analysis, whereas oscillatory-based functional connectivity investigation, particularly in semantic processing is sparse. Therefore, future studies are needed to shed more light on the role of gamma band oscillations in the inter-regional communication during semantic prediction.

We also observed increased alpha band PLVs in the 0–300 ms time window for LP, as compared with HP nouns, between right MTG and right IFG. We interpret these as bottom–up connections in agreement with Schoffelen et al. (2017), who found using granger causality connections originating from temporal areas to peak also at the alpha frequency range. Similarly, Cope et al. (2017) demonstrated causal connections from temporal to frontal areas in alpha band in a speech perception task. The relatively early time window (0–300 ms) and the stronger PLVs within the alpha band for the LP condition further supports the view of bottom–up information transfer. Further studies are required to estimate the direction of information transfer between cortical areas in semantic prediction using, for example, electrocorticogram (ECoG) data offering significant higher signal to noise ratio (Fontolan, Morillon, Liegeois-Chauvel, & Giraud, 2014).

Contextual information available in predictive verbs, coming before HP nouns, allows for the generation of constraining predictions about the upcoming noun and hence pre-activation of aspects of the semantic features of the upcoming noun (Maess et al., 2016; Wang et al., 2012). We hypothesized that this predictive information is available for HP noun processing in the early time window (<200 ms) and tested whether it is represented in gamma power. Out of 7 tested areas, the anterior part of left STG and MTG showed larger gamma power for HP than LP nouns. Increased gamma band power in HP compared with LP words within a sentence is previously reported by (Obleser & Kotz, 2011). In parallel, Lau, Gramfort, Hamalainen, and Kuperberg (2013) have found left anterior temporal cortex to facilitate top–down expectation in lexical semantic prediction in fMRI and MEG experiments. In addition, anterior temporal cortex activation has been found, in response to adjectives, that related to their predictive information on subsequent nouns (Fruchter, Linzen, Westerlund, & Marantz, 2015). In combination, greater gamma power of HP nouns, compared with LP, in left anterior temporal cortex may indicate that low and mid gamma oscillations are involved in the comparison of the prediction and the actual input (Grossberg, 2013; Grossberg & Seidman, 2006; Herrmann, Munk, & Engel, 2004). This is consistent with the proposed model of Lewis and Bastiaansen (2015). This idea is further supported by a recent study (Wang, Hagoort, & Jensen, 2018) demonstrating that gamma power is more strongly correlated, between noun prediction and the actual processing of the noun, when the prediction matches the subsequently processed word, as opposed to when the prediction is violated.

Our hypothesis of more processing in LP, as compared with HP nouns, and increased power in HP rather than LP nouns may seem incongruent. To further clarify, it is helpful to note that more processing in LP nouns may include more processing at most ROIs and especially more inter-regional communication between ROIs. The latter is because the network is certainly more active during LP nouns. Interestingly, we found larger gamma power in the anterior temporal area for HP compared with LP nouns in the very early time interval (<200 ms). This is the time interval during which the prediction is confirmed by the actual input within the lower hierarchical ROIs. Communication within the network remains at a low level in HP noun, though. Therefore, in a later time window (>250 ms), we found increased PLVs in LP compared with HP nouns.

Lastly, there are numerous studies on the functional segregation of N400 neural sources (Friederici, 2002; Hagoort, 2008; Halgren et al., 2002; Jung-Beeman, 2005; Kujala, Alho, Service, Ilmoniemi, & Connolly, 2004; Lau et al., 2008; Maess, Herrmann, Hahne, Nakamura, & Friederici, 2006; Maess et al., 2016). However, studies on the oscillatory dynamics of functional connections underlying this effect are quite sparse. Mellem, Friedman, and Medvedev (2013) found greater coherence between anterior and posterior EEG sensors for unrelated conditions, relative to related, in the theta band over the time windows 150–425 ms and 600–900 ms. It is worth noting that sensor level coherence estimates have the disadvantage of being more prone to produce spurious results than source-level estimates (Schoffelen & Gross, 2009) and also leave the cortical origins of the effects ambiguous. Thus, our article is among the first to present direct oscillatory representations of functional connectivity during N400 generation.

5 | CONCLUSION

In summary, we investigated functional connectivity modulation during a classic N400 paradigm in which identical target nouns were either less predicted (LP) or highly predicted (HP) in simple sentences. Normalized phase-locking values of LP relative to HP were estimated between relevant temporal and frontal ROIs. We found that functional connectivity increased for LP compared with HP nouns in general and in three specific connections: left LOF–left STG within beta and low gamma, right IFG–right MTG within alpha, and left LOF–right IFG within beta band. This is consistent with predictive coding theory,

which proposes reduced information flow between hierarchically organized cortical areas for an HP in contrast to an LP target word. We found increased beta band phase-locking value between left LOF and left STG as well as left LOF and right IFG in LP compared with HP nouns, which is in agreement with a recent hypothesis of beta band involvement in top–down processing. Lastly, low gamma band power was increased for HP compared with LP nouns during an early time window of processing in left anterior temporal cortex, supporting the idea that low gamma oscillations may mediate the matching between the prediction and the input.

ACKNOWLEDGMENTS

This research was supported by the Max Planck Society (ADF, JO, BM, FM), the International Max Planck Research School Leipzig (FM), Nancy Lurie Marks Family Foundation (SK) and Elekta Oy, Finland. We thank Yvonne Wolff for her help in acquiring the data and Joshua Grant for proofreading of the manuscript.

CONFLICT OF INTEREST

The authors declare that they have no conflicts of interest.

ORCID

Fahimeh Mamashli https://orcid.org/0000-0002-7024-943X

REFERENCES

Ahlfors, S. P., Han, J., Belliveau, J. W., & Hamalainen, M. S. (2010). Sensitivity of MEG and EEG to source orientation. *Brain Topography*, *23*, 227–232.

Arnal, L. H., & Giraud, A. L. (2012). Cortical oscillations and sensory predictions. *Trends in Cognitive Sciences*, *16*, 390–398.

Arnal, L. H., Wyart, V., & Giraud, A. L. (2011). Transitions in neural oscillations reflect prediction errors generated in audiovisual speech. *Nature Neuroscience*, *14*, 797.

Badre, D., Poldrack, R. A., Pare-Blagoev, E. J., Insler, R. Z., & Wagner, A. D. (2005). Dissociable controlled retrieval and generalized selection mechanisms in ventrolateral prefrontal cortex. *Neuron*, *47*, 907–918.

Badre, D., & Wagner, A. D. (2007). Left ventrolateral prefrontal cortex and the cognitive control of memory. *Neuropsychologia*, *45*, 2883–2901.

Bastos, A. M., Usrey, W. M., Adams, R. A., Mangun, G. R., Fries, P., & Friston, K. J. (2012). Canonical microcircuits for predictive coding. *Neuron*, *76*, 695–711.

Bastos, A. M., Vezoli, J., Bosman, C. A., Schoffelen, J. M., Oostenveld, R., Dowdall, J. R., … Fries, P. (2015). Visual areas exert feedforward and feedback influences through distinct frequency channels. *Neuron*, *85*, 390–401.

Cannon, J., McCarthy, M. M., Lee, S., Lee, J., Borgers, C., Whittington, M. A., & Kopell, N. (2014). Neurosystems: Brain rhythms and cognitive processing. *The European Journal of Neuroscience*, *39*, 705–719.

Clark, A. (2013). The many faces of precision (replies to commentaries on "whatever next? Neural prediction, situated agents, and the future of cognitive science"). *Frontiers in Psychology*, *4*, 270.

Cope, T. E., Sohoglu, E., Sedley, W., Patterson, K., Jones, P. S., Wiggins, J., … Rowe, J. B. (2017). Evidence for causal top-down frontal contributions to predictive processes in speech perception. *Nature Communications*, *8*, 2154.

David, O., & Friston, K. J. (2003). A neural mass model for MEG/EEG: Coupling and neuronal dynamics. *NeuroImage*, *20*, 1743–1755.

David, O., Maess, B., Eckstein, K., & Friederici, A. D. (2011). Dynamic causal modeling of subcortical connectivity of language. *The Journal of Neuroscience: The Official Journal of the Society for Neuroscience*, *31*, 2712–2717.

DeLong, K. A., Urbach, T. P., & Kutas, M. (2005). Probabilistic word preactivation during language comprehension inferred from electrical brain activity. *Nature Neuroscience*, *8*, 1117–1121.

Doesburg, S. M., Kitajo, K., & Ward, L. M. (2005). Increased gamma-band synchrony precedes switching of conscious perceptual objects in binocular rivalry. *Neuroreport*, *16*, 1139–1142.

Engel, A. K., & Fries, P. (2010). Beta-band oscillations--signalling the status quo? *Current Opinion in Neurobiology*, *20*, 156–165.

Engel, A. K., Fries, P., & Singer, W. (2001). Dynamic predictions: Oscillations and synchrony in top-down processing. *Nature Reviews. Neuroscience*, *2*, 704–716.

Federmeier, K. D. (2007). Thinking ahead: The role and roots of prediction in language comprehension. *Psychophysiology*, *44*, 491–505.

Federmeier, K. D., & Kutas, M. (1999). A rose by any other name: Long-term memory structure and sentence processing. *Journal of Memory and Language*, *41*, 469–495.

Felleman, D. J., & Van Essen, D. C. (1991). Distributed hierarchical processing in the primate cerebral cortex. *Cerebral Cortex*, *1*, 1–47.

Fischl, B., Sereno, M. I., & Dale, A. M. (1999). Cortical surface-based analysis. II: Inflation, flattening, and a surface-based coordinate system. *NeuroImage*, *9*, 195–207.

Fischl, B., Sereno, M. I., Tootell, R. B., & Dale, A. M. (1999). High-resolution intersubject averaging and a coordinate system for the cortical surface. *Human Brain Mapping*, *8*, 272–284.

Fontolan, L., Morillon, B., Liegeois-Chauvel, C., & Giraud, A. L. (2014). The contribution of frequency-specific activity to hierarchical information processing in the human auditory cortex. *Nature Communications*, *5*, 4694.

Friederici, A. D. (2002). Towards a neural basis of auditory sentence processing. *Trends in Cognitive Sciences*, *6*, 78–84.

Friederici, A. D. (2011). The brain basis of language processing: From structure to function. *Physiological Reviews*, *91*, 1357–1392.

Fries, P. (2005). A mechanism for cognitive dynamics: Neuronal communication through neuronal coherence. *Trends in Cognitive Sciences*, *9*, 474–480.

Fries, P. (2015). Rhythms for cognition: Communication through coherence. *Neuron*, *88*, 220–235.

Friston, K. (2005). A theory of cortical responses. *Philosophical Transactions of The Royal Society B Biological Sciences*, *360*, 815–836.

Friston, K., Kilner, J., & Harrison, L. (2006). A free energy principle for the brain. *Journal of Physiology, Paris*, *100*, 70–87.

Fruchter, J., Linzen, T., Westerlund, M., & Marantz, A. (2015). Lexical Preactivation in basic linguistic phrases. *Journal of Cognitive Neuroscience*, *27*, 1912–1935.

Gagnepain, P., Henson, R. N., & Davis, M. H. (2012). Temporal predictive codes for spoken words in auditory cortex. *Current Biology*, *22*, 615–621.

Gramfort, A., Luessi, M., Larson, E., Engemann, D. A., Strohmeier, D., Brodbeck, C., … Hamalainen, M. S. (2014). MNE software for processing MEG and EEG data. *NeuroImage*, *86*, 446–460.

Grisoni, L., Miller, T. M., & Pulvermuller, F. (2017). Neural correlates of semantic prediction and resolution in sentence processing. *The Journal of Neuroscience*, *37*, 4848–4858.

Grossberg, S. (2013). Adaptive resonance theory: How a brain learns to consciously attend, learn, and recognize a changing world. *Neural Networks*, *37*, 1–47.

Grossberg, S., & Seidman, D. (2006). Neural dynamics of autistic behaviors: Cognitive, emotional, and timing substrates. *Psychological Review*, *113*, 483–525.

Hagoort, P. (2008). The fractionation of spoken language understanding by measuring electrical and magnetic brain signals. *Philosophical Transactions of The Royal Society B Biological Sciences*, *363*, 1055–1069.

Halgren, E., Baudena, P., Heit, G., Clarke, J. M., Marinkovic, K., Chauvel, P., & Clarke, M. (1994). Spatio-temporal stages in face and word processing. 2. Depth-recorded potentials in the human frontal and Rolandic cortices. *Journal of Physiology, Paris*, *88*, 51–80.

Halgren, E., Dhond, R. P., Christensen, N., Van Petten, C., Marinkovic, K., Lewine, J. D., & Dale, A. M. (2002). N400-like magnetoencephalography responses modulated by semantic context, word frequency, and lexical class in sentences. *NeuroImage*, *17*, 1101–1116.

Hämäläinen, M. S., & Sarvas, J. (1987). Feasibility of the homogeneous head model in the interpretation of neuromagnetic fields. *Physics in Medicine and Biology*, *32*, 91–97.

Hayes, M. H. (1996). *Statistical digital signal processing and modeling* (Vol. xv, p. 608). New York, NY: John Wiley & Sons.

Helmholtz, H. (1925). *Treatise on physiological optics: Translated from the 3rd German Ed*. Rochester, NY: Optical Society of America.

Herrmann, C. S., Munk, M. H., & Engel, A. K. (2004). Cognitive functions of gamma-band activity: Memory match and utilization. *Trends in Cognitive Sciences*, *8*, 347–355.

Hickok, G. (2012). The cortical organization of speech processing: Feedback control and predictive coding the context of a dual-stream model. *Journal of Communication Disorders*, *45*, 393–402.

Hickok, G., & Poeppel, D. (2007). The cortical organization of speech processing. *Nature Reviews. Neuroscience*, *8*, 393–402.

Huang, Y. P., & Rao, R. P. N. (2011). Predictive coding. *WIREs Cognitive Science*, *2*, 580–593.

Jakuszeit, M., Kotz, S. A., & Hasting, A. S. (2013). Generating predictions: Lesion evidence on the role of left inferior frontal cortex in rapid syntactic analysis. *Cortex*, *49*, 2861–2874.

Jung-Beeman, M. (2005). Bilateral brain processes for comprehending natural language. *Trends in Cognitive Sciences*, *9*, 512–518.

Kamide, Y., Scheepers, C., & Altmann, G. T. (2003). Integration of syntactic and semantic information in predictive processing: Cross-linguistic evidence from German and English. *Journal of Psycholinguistic Research*, *32*, 37–55.

Khan, S., Gramfort, A., Shetty, N. R., Kitzbichler, M. G., Ganesan, S., Moran, J. M., … Joseph, R. M. (2013). Local and long-range functional connectivity is reduced in concert in autism spectrum disorders. *Proceedings of the National Academy of Sciences of the United States of America*, *110*, 3107–3112.

Khan, S., Hashmi, J. A., Mamashli, F., Michmizos, K., Kitzbichler, M. G., Bharadwaj, H., … Kenet, T. (2018). Maturation trajectories of cortical resting-state networks depend on the mediating frequency band. *NeuroImage*, *174*, 57–68.

Kitzbichler, M. G., Khan, S., Ganesan, S., Vangel, M. G., Herbert, M. R., Hämäläinen, M. S., & Kenet, T. (2015). Altered development and multifaceted band-specific abnormalities of resting state networks in autism. *Biological Psychiatry*, *77*, 794–804.

Knoeferle, P., Crocker, M. W., Scheepers, C., & Pickering, M. J. (2005). The influence of the immediate visual context on incremental thematic role-assignment: Evidence from eye-movements in depicted events. *Cognition*, *95*, 95–127.

Kopell, N., Ermentrout, G. B., Whittington, M. A., & Traub, R. D. (2000). Gamma rhythms and beta rhythms have different synchronization properties. *Proceedings of the National Academy of Sciences of the United States of America*, *97*, 1867–1872.

Kujala, A., Alho, K., Service, E., Ilmoniemi, R. J., & Connolly, J. F. (2004). Activation in the anterior left auditory cortex associated with phonological analysis of speech input: Localization of the phonological mismatch negativity response with MEG. *Brain Research. Cognitive Brain Research*, *21*, 106–113.

Kutas, M., & Federmeier, K. D. (2011). Thirty years and counting: Finding meaning in the N400 component of the event-related brain potential (ERP). *Annual Review of Psychology*, *62*(62), 621–647.

Kutas, M., & Hillyard, S. A. (1980a). Event-related brain potentials to semantically inappropriate and surprisingly large words. *Biological Psychology*, *11*, 99–116.

Kutas, M., & Hillyard, S. A. (1980b). Reading senseless sentences - brain potentials reflect semantic incongruity. *Science*, *207*, 203–205.

Kutas, M., & Hillyard, S. A. (1984). Brain potentials during Reading reflect word expectancy and semantic association. *Nature*, *307*, 161–163.

Lachaux, J. P., Rodriguez, E., Martinerie, J., & Varela, F. J. (1999). Measuring phase synchrony in brain signals. *Human Brain Mapping*, *8*, 194–208.

Lau, E., Almeida, D., Hines, P. C., & Poeppel, D. (2009). A lexical basis for N400 context effects: Evidence from MEG. *Brain and Language*, *111*, 161–172.

Lau, E.F. (2009) The predictive nature of language comprehension. (Dissertation). University of Maryland, College Park, MD.

Lau, E. F., Gramfort, A., Hamalainen, M. S., & Kuperberg, G. R. (2013). Automatic semantic facilitation in anterior temporal cortex revealed through multimodal neuroimaging. *The Journal of Neuroscience*, *33*, 17174–17181.

Lau, E. F., Holcomb, P. J., & Kuperberg, G. R. (2013). Dissociating N400 effects of prediction from association in single-word contexts. *Journal of Cognitive Neuroscience*, *25*, 484–502.

Lau, E. F., Phillips, C., & Poeppel, D. (2008). A cortical network for semantics: (de)constructing the N400. *Nature Reviews. Neuroscience*, *9*, 920–933.

Lewis, A. G., & Bastiaansen, M. (2015). A predictive coding framework for rapid neural dynamics during sentence-level language comprehension. *Cortex*, *68*, 155–168.

Lewis, A. G., Schoffelen, J. M., Schriefers, H., & Bastiaansen, M. (2016). A predictive coding perspective on Beta oscillations during sentence-level language comprehension. *Frontiers in Human Neuroscience*, *10*, 85.

Lin, F. H., Belliveau, J. W., Dale, A. M., & Hämäläinen, M. S. (2006). Distributed current estimates using cortical orientation constraints. *Human Brain Mapping*, *27*, 1–13.

Maess, B., Herrmann, C. S., Hahne, A., Nakamura, A., & Friederici, A. D. (2006). Localizing the distributed language network responsible for the N400 measured by MEG during auditory sentence processing. *Brain Research*, *1096*, 163–172.

Maess, B., Mamashli, F., Obleser, J., Helle, L., & Friederici, A. D. (2016). Prediction signatures in the brain: Semantic pre-activation during language comprehension. *Frontiers in Human Neuroscience*, *10*, 591.

Mamashli, F., Khan, S., Bharadwaj, H., Michmizos, K., Ganesan, S., Garel, K. A., … Kenet, T. (2017). Auditory processing in noise is associated with complex patterns of disrupted functional connectivity in autism spectrum disorder. *Autism Research*, *10*, 631–647.

Maris, E., & Oostenveld, R. (2007). Nonparametric statistical testing of EEG- and MEG-data. *Journal of Neuroscience Methods*, *164*, 177–190.

Maris, E., Schoffelen, J. M., & Fries, P. (2007). Nonparametric statistical testing of coherence differences. *Journal of Neuroscience Methods*, *163*, 161–175.

Martin, A. (2007). The representation of object concepts in the brain. *Annual Review of Psychology*, *58*, 25–45.

McRae, K., Hare, M., Elman, J. L., & Ferretti, T. (2005). A basis for generating expectancies for verbs from nouns. *Memory & Cognition*, *33*, 1174–1184.

Mellem, M. S., Friedman, R. B., & Medvedev, A. V. (2013). Gamma- and theta-band synchronization during semantic priming reflect local and long-range lexical-semantic networks. *Brain and Language*, *127*, 440–451.

Mumford, D. (1992). On the computational architecture of the neocortex .2. The role of corticocortical loops. *Biological Cybernetics*, *66*, 241–251.

Obleser, J. (2016). Tell me something I don't know. *eLife*, *5*, e15853.

Obleser, J., & Kotz, S. A. (2011). Multiple brain signatures of integration in the comprehension of degraded speech. *NeuroImage*, *55*, 713–723.

Oldfield, R. C. (1971). The assessment and analysis of handedness: The Edinburgh inventory. *Neuropsychologia*, *9*, 97–113.

Omoigui, N., He, L., Grudin, J., Sanocki, E. (1999) Time compression: Systems, concerns, usage, and benefits. ACM CHI'99. Pittsburg, PA.

Panagiotaropoulos, T. I., Deco, G., Kapoor, V., & Logothetis, N. K. (2012). Neuronal discharges and gamma oscillations explicitly reflect visual consciousness in the lateral prefrontal cortex. *Neuron*, *74*, 924–935.

Pantazis, D., Fang, M., Qin, S., Mohsenzadeh, Y., Li, Q., & Cichy, R. M. (2017). Decoding the orientation of contrast edges from MEG evoked and induced responses. *NeuroImage*, *180*, 267–297.

Park, H., Ince, R. A., Schyns, P. G., Thut, G., & Gross, J. (2015). Frontal top-down signals increase coupling of auditory low-frequency oscillations to continuous speech in human listeners. *Current Biology*, *25*, 1649–1653.

Price, C. J. (2010). The anatomy of language: A review of 100 fMRI studies published in 2009. *Annals of the New York Academy of Sciences*, *1191*, 62–88.

Pylkkanen, L., & Marantz, A. (2003). Tracking the time course of word recognition with MEG. *Trends in Cognitive Sciences*, *7*, 187–189.

Rao, R. P. N., & Ballard, D. H. (1999). Predictive coding in the visual cortex: A functional interpretation of some extra-classical receptive-field effects. *Nature Neuroscience*, *2*, 79–87.

Schoffelen, J. M., & Gross, J. (2009). Source connectivity analysis with MEG and EEG. *Human Brain Mapping*, *30*, 1857–1865.

Schoffelen, J. M., Hulten, A., Lam, N., Marquand, A. F., Udden, J., & Hagoort, P. (2017). Frequency-specific directed interactions in the

human brain network for language. *Proceedings of the National Academy of Sciences of the United States of America*, *114*, 8083–8088.

Scott, S. K., Blank, C. C., Rosen, S., & Wise, R. J. S. (2000). Identification of a pathway for intelligible speech in the left temporal lobe. *Brain*, *123*, 2400–2406.

Sedley, W., Gander, P. E., Kumar, S., Kovach, C. K., Oya, H., Kawasaki, H., … Griffiths, T. D. (2016). Neural signatures of perceptual inference. *eLife*, *5*, e11476.

Sekihara, K., Owen, J. P., Trisno, S., & Nagarajan, S. S. (2011). Removal of spurious coherence in MEG source-space coherence analysis. *IEEE Transactions on Bio-medical Engineering*, *58*, 3121–3129.

Sohoglu, E., Peelle, J. E., Carlyon, R. P., & Davis, M. H. (2012). Predictive top-down integration of prior knowledge during speech perception. *The Journal of Neuroscience*, *32*, 8443–8453.

Srinivasan, M. V., Laughlin, S. B., & Dubs, A. (1982). Predictive coding: A fresh view of inhibition in the retina. *Proceedings of the Royal Society of London - Series B: Biological Sciences*, *216*, 427–459.

Stoica, P., & Moses, R. L. (1997). *Introduction to spectral analysis* (Vol. xviii, p. 319). Upper Saddle River, NJ: Prentice Hall.

Swanson, L. R. (2016). The predictive processing paradigm has roots in Kant. *Frontiers in Systems Neuroscience*, *10*, 79.

Tallon-Baudry, C., & Bertrand, O. (1999). Oscillatory gamma activity in humans and its role in object representation. *Trends in Cognitive Sciences*, *3*, 151–162.

Taulu, S., Kajola, M., & Simola, J. (2004). Suppression of interference and artifacts by the signal space separation method. *Brain Topography*, *16*, 269–275.

Taulu, S., & Simola, J. (2006). Spatiotemporal signal space separation method for rejecting nearby interference in MEG measurements. *Physics in Medicine and Biology*, *51*, 1759–1768.

Taylor, W. L. (1953). "Cloze procedure": A new tool for measuring readability. *Journalism Quarterly*, *30*, 415–433.

Thompson-Schill, S. L., D'Esposito, M., & Kan, I. P. (1999). Effects of repetition and competition on activity in left prefrontal cortex during word generation. *Neuron*, *23*, 513–522.

Van den Brink, D., Brown, C. M., & Hagoort, P. (2001). Electrophysiological evidence for early contextual influences during spoken-word recognition: N200 versus N400 effects. *Journal of Cognitive Neuroscience*, *13*, 967–985.

Van Essen, D. C., & Dierker, D. L. (2007). Surface-based and probabilistic atlases of primate cerebral cortex. *Neuron*, *56*, 209–225.

Van Petten, C., Coulson, S., Rubin, S., Plante, E., & Parks, M. (1999). Time course of word identification and semantic integration in spoken language. *Journal of Experimental Psychology. Learning, Memory, and Cognition*, *25*, 394–417.

Wang, L., Hagoort, P., & Jensen, O. (2018). Gamma oscillatory activity related to language prediction. *Journal of Cognitive Neuroscience*, *30*, 1–12.

Wang, L., Zhu, Z. D., & Bastiaansen, M. (2012). Integration or predictability? A further specification of the functional role of gamma oscillations in language comprehension. *Frontiers in Psychology*, *3*, 187.

Wang, X. J. (2010). Neurophysiological and computational principles of cortical rhythms in cognition. *Physiological Reviews*, *90*, 1195–1268.

Weeks, R. A., Aziz-Sultan, A., Bushara, K. O., Tian, B., Wessinger, C. M., Dang, N., … Hallett, M. (1999). A PET study of human auditory spatial processing. *Neuroscience Letters*, *262*, 155–158.

Wlotko, E. W., & Federmeier, K. D. (2012). So that's what you meant! Event-related potentials reveal multiple aspects of context use during construction of message-level meaning. *NeuroImage*, *62*, 356–366.

How to cite this article: Mamashli F, Khan S, Obleser J, Friederici AD, Maess B. Oscillatory dynamics of cortical functional connections in semantic prediction. *Hum Brain Mapp*. 2019;40:1856–1866. https://doi.org/10.1002/hbm.24495